AD-A276 550

REPORT DOCUMENTATION PAGE

Form Approved
OMB No 0704-0188

on is estimated to average 1 hour per response, including the time for reviewing instructions, searching existing data sources leting and reviewing the collection of information. Send comments regarding this burden estimate or any other aspect of this ducing this burden to Washington Headquarters Services, Directorate for information Operations and Reports, 1215 Jefferson and to the Office of Management and Budget, Paperwork Reduction Project (0704-0188), Washington, DC 20503

2. REPORT DATE	3. REPORT TYPE AND DATES COVERED
February 1994	Annual Technical Report (2/1/93–1/31/94)

4. TITLE AND SUBTITLE	5. FUNDING NUMBERS
Passive Vibration Damping Materials: Piezoelectric Ceramic Composites for Vibration Damping Applications	Current No. N00014-92-J-1391

6. AUTHOR(S)

Shoko Yoshikawa

7. PERFORMING ORGANIZATION NAME(S) AND ADDRESS(ES)	8. PERFORMING ORGANIZATION REPORT NUMBER
The Pennsylvania State University Materials Research Laboratory University Park, PA 16802	94-07246

9. SPONSORING/MONITORING AGENCY NAME(S) AND ADDRESS(ES)

Office of Naval Research, Code 1131M
Ballston Tower One
800 North Quincy Street
Arlington, VA 22217-5000

DTIC
ELECTE
MAR 0 4 1994
B

11. SUPPLEMENTARY NOTES

N/A

12a. DISTRIBUTION/AVAILABILITY STATEMENT	12b. DISTRIBUTION CODE
Distribution unlimited.	

DISTRIBUTION STATEMENT A
Approved for public release;
Distribution Unlimited

13. ABSTRACT (Maximum 200 words)

The study to produce ultra-fine (less than 50 μm in diameter) lead zirconate titanate (PZT) ceramic fibers for passive damping application has been carried out under several aspects. Sol-gel chemistry was undertaken to produce stable spinnable sol, as well as high quality PZT fibers. Due to the extreme geometry of such fibers, special characterization and poling methods were established. Single fiber dielectric properties, polarization hysteresis, and mechanical properties have been measured. Several methods for applying optimum resistive coatings were also explored. The analytical model of passively damped polymer composites using resistively shunted piezoelectric fiber was further developed to predict the behavior of such composites.

14. SUBJECT TERMS	15. NUMBER OF PAGES
Shunted passive piezoelectric damping, PZT sol-gel fiber.	32
	16. PRICE CODE

17. SECURITY CLASSIFICATION OF REPORT	18. SECURITY CLASSIFICATION OF THIS PAGE	19. SECURITY CLASSIFICATION OF ABSTRACT	20. LIMITATION OF ABSTRACT
Unclassified	Unclassified	Unclassified	UL

NSN 7540-01-280-5500

Standard Form 298 (Rev 2-89)
Prescribed by ANSI Std 239-18
298-132

94 3 03 169

GENERAL INSTRUCTIONS FOR COMPLETING SF 298

The Report Documentation Page (RDP) is used in announcing and cataloging reports. It is important that this information be consistent with the rest of the report, particularly the cover and title page. Instructions for filling in each block of the form follow. It is important to *stay within the lines* to meet *optical scanning requirements*.

Block 1. Agency Use Only *(Leave blank)*

Block 2. Report Date. Full publication date including day, month, and year, if available (e.g. 1 Jan 88). Must cite at least the year.

Block 3. Type of Report and Dates Covered. State whether report is interim, final, etc. If applicable, enter inclusive report dates (e.g. 10 Jun 87 - 30 Jun 88).

Block 4. Title and Subtitle. A title is taken from the part of the report that provides the most meaningful and complete information. When a report is prepared in more than one volume, repeat the primary title, add volume number, and include subtitle for the specific volume. On classified documents enter the title classification in parentheses.

Block 5. Funding Numbers. To include contract and grant numbers; may include program element number(s), project number(s), task number(s), and work unit number(s). Use the following labels:

C	- Contract	PR	- Project
G	- Grant	TA	- Task
PE	- Program Element	WU	- Work Unit Accession No.

Block 6. Author(s). Name(s) of person(s) responsible for writing the report, performing the research, or credited with the content of the report. If editor or compiler, this should follow the name(s).

Block 7. Performing Organization Name(s) and Address(es). Self-explanatory.

Block 8. Performing Organization Report Number. Enter the unique alphanumeric report number(s) assigned by the organization performing the report.

Block 9. Sponsoring/Monitoring Agency Name(s) and Address(es). Self-explanatory.

Block 10. Sponsoring/Monitoring Agency Report Number. *(If known)*

Block 11. Supplementary Notes. Enter information not included elsewhere such as: Prepared in cooperation with...; Trans. of...; To be published in.... When a report is revised, include a statement whether the new report supersedes or supplements the older report.

Block 12a. Distribution/Availability Statement. Denotes public availability or limitations. Cite any availability to the public. Enter additional limitations or special markings in all capitals (e.g. NOFORN, REL, ITAR).

DOD	- See DoDD 5230.24, "Distribution Statements on Technical Documents."
DOE	- See authorities.
NASA	- See Handbook NHB 2200.2.
NTIS	- Leave blank.

Block 12b. Distribution Code.

DOD	- Leave blank.
DOE	- Enter DOE distribution categories from the Standard Distribution for Unclassified Scientific and Technical Reports.
NASA	- Leave blank.
NTIS	- Leave blank.

Block 13. Abstract. Include a brief *(Maximum 2...) words)* factual summary of the most significant information contained in the report.

Block 14. Subject Terms. Keywords or phrases identifying major subjects in the report.

Block 15. Number of Pages. Enter the total number of pages.

Block 16. Price Code. Enter appropriate price code *(NTIS only)*.

Blocks 17. - 19. Security Classifications. Self-explanatory. Enter U.S. Security Classification in accordance with U.S. Security Regulations (i.e., UNCLASSIFIED). If form contains classified information, stamp classification on the top and bottom of the page.

Block 20. Limitation of Abstract. This block must be completed to assign a limitation to the abstract. Enter either UL (unlimited) or SAR (same as report). An entry in this block is necessary if the abstract is to be limited. If blank, the abstract is assumed to be unlimited.

"PASSIVE VIBRATION DAMPING MATERIALS: PIEZOELECTRIC CERAMIC COMPOSITES FOR VIBRATION DAMPING APPLICATION"

TO:

DEPARTMENT OF THE NAVY
OFFICE OF NAVAL RESEARCH

FROM:

Shoko Yoshikawa
Materials Research Laboratory
The Pennsylvania State University

CONTRIBUTORS:

R. Meyer, P. Moses, T. Shrout, and J. Witham
Materials Research Laboratory

G. Lesieutre and S. Yarlagadda
Aerospace Engineering

February 1994

TABLE OF CONTENTS

1. INTRODUCTION

This project was initiated in January 1990 under ONR's Accelerated Research Initiative "Acoustic Damping Materials" with the purpose of exploring new methods of vibration absorption using a composite system with a ferroic solid as the active phase. The choice of ferroic solid controls the major damping mechanisms, whereas the matrix material provides mechanical strength as well as stress transfer to the active phase.

Our choice for the active phase is a piezoelectric ceramic material, lead zirconate titanate (PZT). The principle of shunted passive piezoelectric damping was demonstrated using PZT ceramics in both theory and experiment during the first and second years of the contract under Grant No. N00014-90-1540.[1,2] In passive energy dissipation applications, the electrodes of the piezoelectric ceramics are shunted with some electric conductance, hence the term "shunted piezoelectric".

The third year's effort, starting under current contract No. N00014-92-J-1391, was directed at studying the ways in which PZT fibers could be incorporated into structural materials to achieve shunted piezoelectric damping. Fine PZT tubes (1.2 mm in diameter), which are commercially available, were obtained to demonstrate PZT incorporation in structural materials. One of the first methods tried was two-tube PZT modules in a polymer matrix with external resistance. Another approach was to produce PZT tubes in a glass-fiber reinforced epoxy.

One of the most practical methods for large-scale production of structural polymeric materials is to use piezoelectric ceramics in fiber form, which must have high electro-mechanical coupling and must have diameters that are comparable to those of reinforcing fiber materials used in the structural composites. The demonstration of sol -gel derived $PbTiO_3$ and PZT fiber[3,4] indicated that the sol-gel route is the optimum method for producing sub-100 μm diameter piezoelectric ceramic fibers.

The third and fourth years' (this report period) effort, therefore, was aimed at producing fine PZT fibers by the sol-gel method, at optimizing this sol-gel process, and at establishing methods to pole and to characterize such fine fibers with diameters less than 100 μm.

A portion of the effort was also aimed at establishing modeling methods to estimate the achievable damping levels, the shape of frequency-dependence, and the effects of complex stress states and shunting network topology.

2. ACHIEVEMENTS FOR THE PERIOD FROM FEBRUARY 1, 1993 TO JANUARY 31, 1994

The achievements in this period were multifaceted. First, in order to consistently produce PZT fibers, a study for understanding and controlling the mechanisms for PZT sol-gel transition was undertaken. Secondly, independent from the sol-gel fiber formation study, the method to characterize fine PZT fibers had to be established to understand their properties. Third, the method for continuously poling fine PZT fibers without applying electrodes was established. Fourth, area with the conjunction with theory, the methods necessary to apply a resistive coating on the fiber is to explored. The experiment was performed using PZT plates to determine the conditions. Lastly, modeling of resistively shunted PZT embedded composites has been developed to describe the behavior as well as to be a tool for design of such composites.

2.1. Sol-Gel Chemistry and Fiber Formation

With the help of the ONR's AASERT (Augmentation Awards for Science and Engineering Research Training) support, a student has been looking into the effects of additives and the processing conditions on the sol-gel transition and the fiber drawing ability.

In order to understand the factors that affect the gelation of organically derived solutions, it is necessary to develop a systematic scheme to isolate a particular variable. The variables in question can then be studied by altering the processes involved. The following are a number of variables which are influential on the quality of the solution itself:

a. Selection of precursors
b. Hydrolysis/humidity
c. pH/acid addition
d. Others

The sol-gel transition is accompanied by a rapid change in viscosity and rheological behavior. The transition, or T_{gel}, is defined as when the last bond is formed between large interconnected networks, forming a continuous network throughout the sample. This last bond is no different from any other bond in the system; however, it is the first bond to give the whole body elasticity. At this point, the mass is referred to as a wet gel. In a wet gel, there are two continuous networks: polymer chains and a liquid phase. The liquid phase comprising the gel at T_{gel} is considered to have almost equivalent transport properties as a pure liquid. Also, it has been shown that the rate of evaporation from a wet gel and a pure liquid is equal. As the gel dries, synthesis

2

continues and large capillary pressures build. T_{gel} in fiber drawing would be the point at which sol loses its ability to form a fiber.

The viscosity of the sol is important in fiber drawing. Through the sol-gel transition, there is an exponential increase in viscosity. Initially, the viscosity ranges from 1 to 20 cp and only increases slightly with the polymerization until the gel point nears. As the condensation reaction continues, the polymer chains begin to become entangled and crosslinked, connecting independent polymer clusters. This results in an exponential rise in viscosity. The rise in viscosity must be controlled to optimize fiber drawing. The exact viscosity in the fiber drawing region has not yet been determined. It is important to have a viscous solution to pull a fiber and retain its shape after it has been drawn.

The rheological behavior of the sol also changes during the sol-gel transition. The initial sol is composed mainly of solvent and additives, plus the polymer components which are only a few atoms in length. Thus, the sol should exhibit a Newtonian behavior. Once the network chains begin to crosslink and start to become entangled, the rheological properties change to a shear thinning or a pseudoplastic behavior. The best fiber drawing sols (drawn using a glass rod) display Newtonian or pseudoplastic, whereas the sols that exhibit shear thinning are unsuitable for drawing fibers. It is possible to obtain a network structure that has a constant viscosity with increasing shear rate. This occurs if the polymer is linear with very little crosslinking, which usually happens under acidic conditions.

Currently the experiments are being carried out: (1) vary the amount of water per mole of PZT starting at 1:1 H_2O:PZT, (2) vary the temperature (room temp., 40, 60, and 80°C), and (3) repeat (1) and (2) varying the amount of acid (HNO_3) added during curing starting at 1:1.

The results of the above experiments are intended to be summarized in the AASERT annual report in June 94.

2.2. PZT Fiber Characterization Methods

A special fixture was built to measure dielectric and polarization properties of single PZT fibers. A special tool was also used to determine mechanical tensile strength of the sol-gel derived PZT fibers. It was found that the sol-gel derived PZT fibers fired at 1250°C with an average diameter of 30 μm have similar dielectric constant, polarization hysteresis, and mechanical properties to those of bulk PZT ceramics. A detailed report on the characterization methods, results and discussion is found in the published proceedings attached in Appendix A.

3

2.3. Fiber Poling Method

Lead zirconate titanate (PZT) ceramics, unlike single-crystal piezoelectric materials such as quartz or Rochelle salt, are polycrystalline materials, which consist of a multitude of tiny, piezoelectric crystallites at random orientation. This random orientation causes the overall ceramic to be inactive, with no piezoelectricity detectable until some means is found to polarize the ceramic as a whole entity. The decisive step here is the poling process: that is, application of a high voltage sufficient to reverse the electric moments of spontaneously polarized regions in the ceramic.

Almost all of the piezoelectric composites consisting of PZT ceramic and an insulating matrix, such as polymer, have been poled after the composite formation is completed. This, however, limits the thickness (distance between electrodes) of the composite to less than 1 cm, since the typical required poling field for PZT is between 10 to 30 kV/cm. It also requires the electrode coating on the entire surface as shown in the shaded area of the composites in Fig. 1.

PARTICLES IN A POLYMER

PZT RODS IN A POLYMER

PZT SPHERES IN A POLYMER
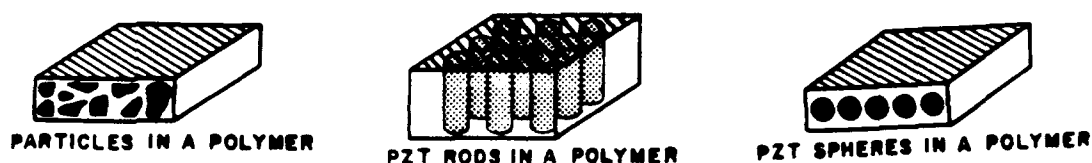
Figure 1. **Schematic diagram of some types of PZT composites with electroded surface (shaded area, only top surface is shown).**

It has been proven that the most efficient piezoelectric passive damping is achieved by using k_{33} coupling coefficient of PZT, which would have the fiber poled in length direction and the stress applied to the same direction[1,2]. Therefore, the attempts have been made to pole these fine fibers in longitudinal direction before the incorporation into the matrix. In addition, for the passive damping applications, incorporation of already poled fibers will permit us to produce large size composites for structural materials.

Prior art describing continuous poling[3] required close contact of the electrode with PZT ceramic. The method described in last year's technical report[4] also that the required conductive rubber ring be in contact with the PZT fiber. Due to the fragile nature of the fine PZT fibers, this method was not feasible. Therefore, based on the limiting conditions that a large amount of fibers need to be poled simultaneously and continuously and that the fine fibers, although retaining the

mechanical properties of bulk PZT, are rather fragile, a new poling method was attempted, and it showed initial success. Nonetheless, the fibers used for this experiment were extruded PZT-5H (120 μm in diameter) obtained from CeraNova Corp. for the ease of handling, instead of sol-gel derived PZT fiber.

Fig. 2 describes the poling PZT fibers in which PZT fiber is threaded through two small holes (0.45 mm diameter), one hole in a large stainless steel sphere (10 cm diameter), and the other in a large metal plate (25 cm^2), 2 to 4 cm apart. With the plate at ground potential, the sphere is gradually raised to sufficient voltage to significantly exceed the coercive field of the PZT. The high voltage side is at the sphere in order to reduce the breakdown and corona effects that exist at the edge of a plate.
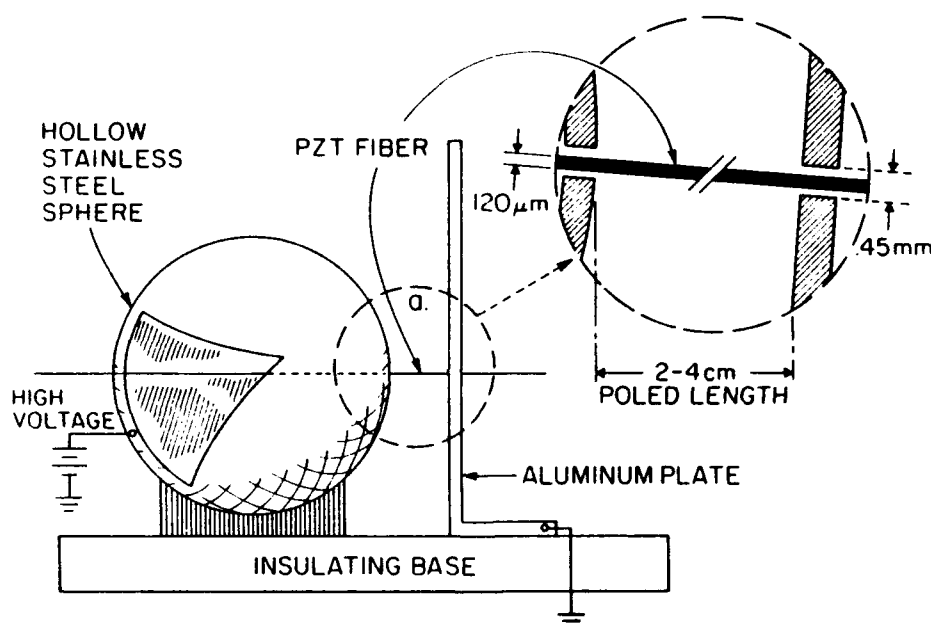
Figure 2. Fiber poling apparatus

The fiber segment, where the 30 kV/cm field was applied between the sphere and plates in air, showed a nearly complete shift of the first hysteresis loop, which indicates that the fiber has been poled.

Since the voltage is slowly raised compared to the charging times involved, it is considered to be the static field case. In this case, the electric field in and around the fiber is nearly uniform The only perturbations from uniformity are caused by the small holes in the plates and the spherical geometry of the high voltage side. Yet the holes are quite small compared to the separation distance and the diameters of the plates; thus they do not significantly affect the field. As the voltage is raised, most of the fiber is forced to experience the field between the sphere and the

5

plate. In the area where the fiber is threaded in the holes, the field must be curving radially outward, but this is a very short zone, on the same order as the hole diameter.

The majority of the fiber should be subjected to a longitudinal field, which could pole the fiber; except that as the field in the fiber approaches the coercive field, significant charge separation occurs. There has to be a mechanism to draw off that charge, or it would tend to cancel the applied field. This is the reason for not being able to pole a bulk PZT with non-contacting electrodes. In this case, however, the charge starts to accumulate in a ring where the fiber is threaded.

There are several assumptions as to how this charge is dissipated in the experiments:

1. Corona formation from the surface of the sample to the sharp edge of metal forming the circumference of the hole where the fiber is threaded through.
2. Air breakdown caused in the same way a corona is formed.
3. Conduction through the fiber, possibly along grain boundaries.
4. Surface conduction driven by the high field of case 3.

The one problem with this method is that the air between the plate and sphere tends to break down. Poling at an elevated temperature will not only be able to increase the breakdown strength but also make the poling of PZT relatively easier.

2.4. Resistive coating

According to our calculations (found in 2-5 Modeling section), the realistic range for the fiber coating resistivity is 10^4 to 10^6 Ωcm, assuming 1 mm-coating thickness on the 30 μm diameter PZT fibers so as to damp a frequency of less than 100 Hz.

The conditions required for the coating process and materials are:
1. Lower substrate (PZT) temperature to avoid depoling
2. Shorter exposure to vacuum to avoid reduction of PZT surface
3. Easy resistivity control
4. Stable in environment and compatible with host material (polymer)
5. Lower cost

Various kinds of metal targets can be used to produce controlled resistive coatings in the form of metal oxides by sputtering or deposition techniques. As an initial trial, microwave plasma deposition of an Al_2O_3 coating using an Al target was tried on several flat bulk PZT substrates. Surface resistance for a 0.7 μm coating was over 10^9 Ω, which was calculated to be a resistivity of

6

$\geq 10^4$ Ω cm. By increasing deposition time and deposition rate, a coating thickness of 1.97 μm was obtained. Due to the constraints of the resistivity range and the coating thickness, the coating resistance is in the range which is difficult to measure precisely (resistance value over 10^9 Ω). The measurement technique for this resistance range needs to be carefully established.

Other materials and methods that are available at the Materials Research Laboratory for resistive coating for PZT include magnetron sputtering or arc source vapor deposition of carbon/graphite to diamond-like films. The substrate temperature during the sputtering ranges from room temperature to 60°C. Graphite is an electrical conductor and anisotropic material, in which each atom is sp^2 bonded. Diamond is a hard, wide-band gap semiconductor, in which each atom is 4-fold coordinated and sp^3 bonded. By controlling sp^2 and sp^3 bonding ratio, one can obtain a coating with a certain resistivity value.

If a lower resistivity is required, a layer of metal clusters, such as copper, with a controlled thickness, will provide necessary resistivity. Protective coating (e.g., Al_2O_3) will be needed to prevent oxidation of the metal as shown in Fig. 3.
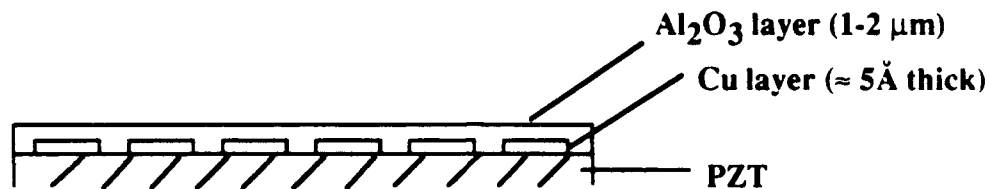
Figure 3. Example of Application of Cu clusters.

2.5. Modeling

The initial modeling effort to provide performance analysis of PZT containing polymer/matrix composite lamina has been summarized in the article in Appendix B.

An analytical model to describe the behavior of polymer matrix composites, which are passively damped using resistively shunted piezoelectric fibers, is developed for enhanced damping performance of the composite. The fibers may (or may not) serve as the sole reinforcement in the composite. Given the structural geometry and mechanical properties of the constituents in the composite, the model should be capable of predicting modal frequencies and damping of the passively damped composite structure.

As a summary, for a one-dimensional case, the two coupled 3-D governing differential equations reduce to one equation of the form $\{\rho\omega^2 - K\}$ $U = 0$, where U is complex mechanical displacement and K is complex stiffness, and loss factor of the domain is calculated as a function

7

of the frequency and material properties. Yet, to be of practical benefit, the model should be able to work in an inverse manner; i.e. given the desired damping and structural frequencies, determine the material parameters such as suitable volume fractions, resistive coating characteristics etc. This model may be used to this effect by calculating peak loss factors and corresponding frequencies for several sets of material parameters. The details are described as follows.

2.5.1. Formulation

The key factors in formulating the model are:

- The composite is made up of fibers embedded in a polymer matrix. The fibers can either be shunted piezoelectric fibers alone, or shunted piezoelectric fibers and reinforcing fibers (graphite, glass etc.). Shunting of the piezoelectric fibers is done by coating the fibers with a resistive material (e.g., 1μm coating on a 30 μm fiber). Shunting in this manner will make use of the electromechanical coupling along the poling direction (k_{33}) of the piezoelectric fiber.

- Treat the entire structural domain as a piezoelectric medium, with the matrix and coating assumed to have zero dielectric and piezoelectric properties. The resistive coating on the piezoelectric fiber is treated as an electrical boundary between the fiber and the matrix.

- The volume fraction of the resistive coating is much smaller than that of the fiber or the matrix and the coating is assumed to play no other role than dissipating electrical energy developed in the piezoelectric fiber. Yet, if necessary, it will be possible to include the mechanical properties of the coating in the overall properties of the composite.

- The quasi-static assumption of the linear piezoelectric theory is valid. It is assumed that phase velocities of electromagnetic waves are much higher (6 orders of magnitude) than those of waves due to structural vibration. The model is focused on the spatial and time-dependent behavior of electric potential and charge distribution within the piezoelectric fiber/resistive coating.

- There are no "electrodes" on the piezoelectric fiber. Instead, the resistive coating on the fiber serves as the external electrical path for charge developed in the piezoelectric fiber. Flow of charge within the resistive coating dissipates energy.

- As the model examines spatial and time-dependent behavior of electric potential and the charge distribution within the piezoelectric fiber, the electric field within the fiber is not assumed to be uniform.

- Multiaxial stress states in the piezoelectric fiber and their effect on the overall energy dissipation will be examined. Models in the literature are restricted to uniaxial stress states in the piezoelectric.

- To describe the electromechanical behavior of the structure, two dependent fields, u (mechanical displacement) and ϕ (electric potential) were defined. Two coupled differential equations governing the spatial and time-dependent behavior of each field were developed.

A simplified domain consisting of a single resistively-shunted piezoelectric fiber in a cylinder of polymer matrix was modeled. The piezoelectric fiber was shunted by coating the fiber with a resistive material. Poling direction of the piezoelectric fiber is along the fiber length. A schematic of the simplified domain is shown in Fig. 4. It consists of a single resistance shunted piezoelectric fiber embedded in a polymer matrix "tube". The matrix is assumed to be isotropic and elastic, and the fiber is assumed to be transversely isotropic. Perfect bonding is assumed between the fiber, the coating, and the matrix. Equations governing the behavior of the domain are formulated in the following section.

2.5.2. Constitutive equations

Treating the entire structural domain as a piezoelectric material, the constitutive equations for the domain (from linear piezoelectric theory) are:

$$\sigma_{ij} = C^E_{ijkl} S_{kl} - e_{kij} E_k$$
$$D_i = e_{ikl} S_{kl} + \varepsilon_{ik} E_k$$

where σ is stress, S is strain (a function of u), E is the electric field (a function of ϕ), and D is the electric displacement. ε are the dielectric permittivities, e are the piezoelectric constants and C^E are the material elastic constants at constant electric field.
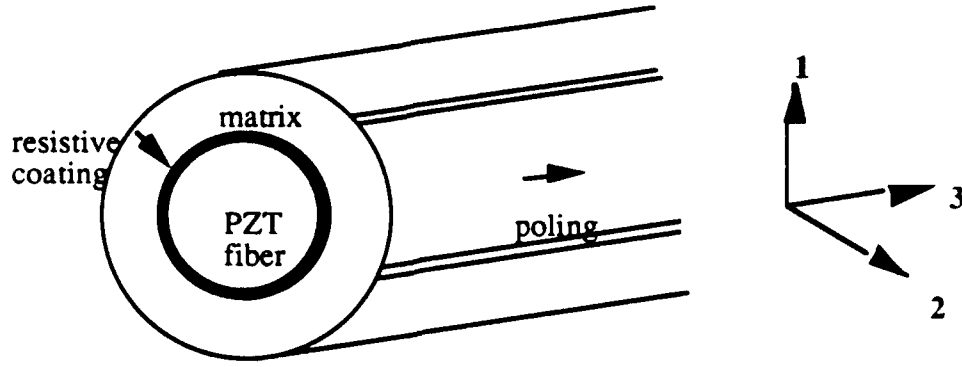
Figure 4. Schematic of the Structural Domain

2.5.3. Time-dependent behavior of u

For a general domain with zero body forces, momentum conservation can be expressed as

$$\sigma_{ij,j} = \rho_0 \, \ddot{u}_i$$

where ρ_0 is the density of the structure. Substituting for the stress σ using the constitutive equation in the preceding equation,

$$C^E_{ijkl} \, u_{k,li} + e_{kij} \, \phi_{,ki} = \rho_0 \, \ddot{u}_j$$

The above equation is a general 3-D differential equation governing the behavior of u and is coupled to ϕ through the piezoelectric constants. Simplifying the above equation to a one dimensional case (along the fiber) and assuming the 3 direction (poling direction) along the fiber direction,

$$C^E_{33} \, u'' + e_{33} \, \phi'' = \rho_0 \, \ddot{u}$$

The material properties in the above equation are the overall domain properties and can be expressed in terms of the constituent properties by any composite micromechanical model. Using Rule-of-Mixtures as a starting point, the domain properties are

10

$$C_{33}^{E} = C_{33_f}^{E}\, v_f + C_{33_m}\, v_m + C_{33_r}\, v_r$$

$$e_{33} = e_{33_f}\, v_f$$

$$\rho_o = \rho_f\, v_f + \rho_m\, v_m + \rho_r\, v_r$$

where v_m, v_f and v_r are volume fractions of the matrix, fiber, and resistive coating respectively.

2.5.4. Time-dependent behavior of ϕ

To understand charge and potential dynamics, charge conservation and Ampere's Law for a general electromagnetic domain are examined.

$$\frac{\partial q}{\partial t} + \nabla \cdot J = 0$$

$$\oint_1 H \cdot dr = \int_s n \cdot \dot{D}\, ds + \int_s n \cdot J\, ds$$

where q is the charge density, J is the current flux, H is the magnetic field intensity and D is the electric displacement. Integration over l and s represent line and surface integrals respectively. For a non-magnetic piezoelectric domain, H is zero. Applying the Divergence theorem to both surface integrals in Ampere's Law,

$$\int_V \nabla \cdot \dot{D}\, dv + \int_V \nabla \cdot J\, dv = 0$$

Differentiating the second constitutive equation with respect to time and with respect to spatial coordinates

$$\nabla \cdot \dot{D}_i = \left(e_{ikl}\, \dot{u}_{l,k} - \varepsilon_{ik}\, \dot{\phi}_{,k} \right)_{,k}$$

The current flux within the domain is restricted to that within the piezoelectric fiber and the resistive coating. Assuming the fiber to be non-conductive (or very high resistance compared to the resistive coating), the current flux J in the domain is

$$J_k = -\sigma_{c_r} v_r \, \phi_{,k}$$

where σ_{c_r} is the electrical conductivity of the resistive coating. Substituting the above equations in the modified form of Ampere's Law,

$$\int_V \left[e_{ikl} \, \dot{u}_{l,k} - \varepsilon_{ik} \, \dot{\phi}_{,k} \right]_{,k} dV + \int_V - \sigma_{c_r} v_r \left[\phi_{,k} \right]_{,k} dV = 0$$

where, in the general case, $k = 1, 2, 3$. The above equation is a 3-D equation governing the spatial and time-dependent behavior of ϕ, which is coupled to u by the piezoelectric constants. The one-dimensional equivalent is

$$e_{33} \, \ddot{u}'' = \varepsilon_{33} \, \dot{\phi}' + \sigma_{c_r} v_r \, \phi''$$

where, as defined previously, the material properties are overall properties of the domain and are expressed in terms of the constitutive properties by the Rule-of-Mixtures as

$$e_{33} = e_{33_f} \, v_f$$
$$\varepsilon_{33} = \varepsilon_{33_f} \, v_f$$

2.5.5. Solution for the one-dimensional case

As formulated in the previous section, the governing equations for the one-dimensional case are

$$C_{33}^E \, u'' + e_{33} \, \phi'' = \rho_o \, \ddot{u}$$

$$e_{33} \, \ddot{u}'' = \varepsilon_{33} \, \dot{\phi}' + \sigma_{c_r} v_r \, \phi''$$

Fourier analysis:

$$u(x,t) = U \, e^{(st + px)}$$

$$\phi(x,t) = \Phi \, e^{(st + px)}$$

Assuming $u(x,t)$ and $\phi(x,t)$ are share temporal and spatial variation, with possible phase shifts. s. p, U, and Φ are complex. Therefore, the second governing equation can be expressed as

$$\Phi = \frac{(e_{33_f} \, v_f) \, s}{(\varepsilon_{33_f} \, v_f \, s + \sigma_{c_r} v_r)} \, U$$

Substituting for u, ϕ and Φ in the first governing equation

$$\left\{ \rho_o \, s^2 - \left[C_{33}^E + \frac{(e_{33_f} \, v_f)^2 \, s}{(\varepsilon_{33_f} \, v_f \, s + \sigma_{c_r} v_r)} \right] p^2 \right\} U = 0$$

The above equation is of the form $\{\rho\omega^2 - K\} \, U = 0$, and the stiffness K is a function of the frequency. This dependence of the overall domain stiffness on the frequency is due to the resistive shunting of the piezoelectric fiber. If the shunt resistance is very high ($\sigma_{c_r} \approx 0$), then there is no frequency dependence. The magnitude of the change in the overall stiffness due to the frequency dependence can be very significant (a factor of 2 in some cases).

For a steady state harmonic vibration, $s = i\omega$. The overall stiffness can be expressed in the following form

$$C_{33}^E(s) = C_{33}^E + \frac{(e_{33_f} v_f)^2 \, s}{(\varepsilon_{33_f} v_f \, s + \sigma_{c_r} v_r)}$$

$$= C_{33}^E \left[1 + \frac{(e_{33_f} v_f)^2}{C_{33}^E(\varepsilon_{33_f} v_f)} \left\{ \frac{(\varepsilon_{33_f} v_f) \, s / \sigma_{c_r} v_r}{1 + (\varepsilon_{33_f} v_f) \, s / \sigma_{c_r} v_r} \right\} \right]$$

Defining,

$$\Delta = \frac{(e_{33_f} v_f)^2}{C_{33}^E(\varepsilon_{33_f} v_f)} \quad , \quad \tau = \frac{(\varepsilon_{33_f} v_f)}{\sigma_{c_r} v_r}$$

and substituting for s, we obtain

$$C_{33}^E(\omega) = C_{33}^E \left[1 + \Delta \frac{\tau(i\omega)}{1 + \tau(i\omega)} \right]$$

$$= C_{33}^E \left[\frac{1 + (1 + \Delta)(\omega\tau)^2}{1 + (\omega\tau)^2} \right] + i \, C_{33}^E \left[\frac{\Delta(\omega\tau)}{1 + (\omega\tau)^2} \right]$$

The frequency dependent stiffness has a complex form as shown above. The real part of the frequency dependent stiffness is the storage modulus and the imaginary part is the loss modulus. The effective loss factor is determined from the ratio of the (loss modulus)/(storage modulus) and is

14

$$\eta = \frac{\Delta(\omega\tau)}{1 + (1 + \Delta)(\omega\tau)^2}$$

The peak damping can be calculated to be

$$\eta_{max} = \frac{\Delta}{2\sqrt{(1 + \Delta)}}$$

2.5.6. Example case

Assuming the following material properties:

C_{33}^E	=	44 GPa
e_{33f}	=	18.8
ε_{33f}	=	5.88 e-9
σ_{c_r}	=	6.2 e-5 $\Omega^{-1}m^{-1}$
vf	=	0.30, $v_r = 0.02$ (1 μm coating on 30 μm diameter fiber)

the peak damping value (η_{max}) obtained is 0.17 at ω = 592 rad/s = 94 Hz.

Changing the resistive coating parameters will change the maximum damping and the corresponding frequency. To use the model as a design tool, the peak damping and corresponding frequency can be calculated for many different coating parameters, volume fractions, etc.

3. FURTHER RESEARCH

The realization of large scale PZT fiber manufacturing depends on the formation of stable spinnable sol as well as other processing issues, such as fiber handling. The concept of resistively shunted PZT for passive damping is well established, and the development of controlled resistive coatings will be a useful tool for even bulk PZT applications. Thus, the various aspects discussed in this report for PZT fiber research will be continued, focusing on sol-gel chemistry and other processing variables.

The next step in modeling is to extend the one-dimensional case to the 2 and 3-D cases of the simplified domain in Fig. 4 to examine the effect of multiaxial stress states. An additional feature that will be examined is a case where the material parameters deviate from the ideal case (for maximum damping), since it is not always possible to achieve the specified design parameters during manufacture of these types of composites.

REFERENCES

1. S.K. Kurtz and S. Yoshikawa, Annual Technical Report to ONR, "Passive Damping" Grant No. N00014-90-J-1540, Jan. 1991.

2. S.K. Kurtz and S. Yoshikawa, Final Technical Report to ONR, "Passive Damping Materials: Piezoelectric Ceramic Composites for Vibration Damping Application," Grant No. N00014-J90-1540, June 1992.

3. T.R. Gururaja, D. Christopher, R.E. Newnham, and W.A. Schulze, "Continuous Poling of PZT Fibers and Ribbons and Its Application to New Devices," Ferroelectrics, 47, 193-200, 1983.

4. S. Yoshikawa, S.K. Kurtz, Annual Technical Report to ONR, "Passive Damping Materials: Piezoelectric Ceramic Composites for Vibration Damping Application," Grant No. N00014-J-92-1391, Feb. 1993.

APPENDIX A

Pb(Zr,Ti)O3 [PZT] FIBERS--FABRICATION AND MEASUREMENT METHODS

Shoko Yoshikawa, Ulagaraj Selvaraj, Paul Moses, and Thomas Shrout
International Center for Actuators and Transducers
Materials Research Laboratory
The Pennsylvania State University
University Park, PA

ABSTRACT

Fine scale lead zirconate titanate (PZT) and niobium substituted PZT (Nb-PZT) piezoelectric fibers were fabricated from sol-gel processed viscous "sol" using the "spinning" methodology developed for the continuous production of glass fibers. Subsequent drying and firing at above 750°C gave pure perovskite PZT and Nb-PZT fibers of 30 μm in average diameter. Further densification and grain growth were evident for fibers fired at 1250°C. Experimental methods for the determination of dielectric and polarization properties were developed to overcome inherent electric field difficulty relevant to fine scale fibers. The dielectric constant and polarization hysteresis values of the fibers were comparable with that of bulk ceramics. Preliminary single fiber mechancial pull tests indicated that the tensile strength of 30 μm diameter PZT fibers were similar to that of bulk ceramics, being in the range of 35-55 MPa.

1. INTRODUCTION

Lead zirconate titanate (PZT) piezoelectric ceramics' ability to efficiently convert electrical energy to mechanical and vice versa has made them attractive for both actuators and sensors in active control systems.[1] This reversible transformation ability also makes piezoceramics viable candidates for passive vibration damping.[2,3] For structural materials comprised of various fibers, i.e. glass and carbon, the incorporation of piezoelectric fibers is, therefore, inherently desired.[4]

Previously, the fabrication of PZT fibers and/or rods has been driven by the need for high performance hydrophones[5] and ultrasonic transducers.[6] In such cases, PZT fibers/rods are fabricated simply by the dicing of bulk ceramics[7], being limited to simple geometries on the order of a few millimeters in length and ~ 100 μm in cross section. Extrusion, the process by which a plasticized ceramic mass is passed through a die or orifice, provides the ability to fabricate meter length fibers with various cross-sectional geometries; however, they are again limited to diameters of ~ 100 μm[8]. For fibers with diameters less than 100 μm, non-conventional methods have been employed, including the impregnation of host fibers with a precursor solution[9] and hand drawing from a viscous sol.[10,11,12] Single strand fibers fabricated thus far have been limited to lengths of a few centimeters, being for demonstration purposes only. Furthermore, little information regarding electrical and mechanical properties has yet to be reported.

It was the objective of this work to fabricate fine-scale PZT fibers using a "spinning" methodology developed for the continuous production of carbon and/or glass fibers. A further objective was to determine the electrical and mechanical properties of individual fibers prepared above.

2. EXPERIMENTAL PROCEDURE

2.1. PZT Fiber Fabrication

The advantages of sol-gel processing in the fabrication of ferroelectric thin films; i.e., compositional control, low-temperature densification and overall simplicity makes it the ideal methodology for the fabrication of fine-scale fibers. In the sol-gel process, a non-aqueous solution of precursors, generally alkoxides, is

prepared with the metal cations in the desired stoichiometry, followed by controlled hydrolysis to form a "sol" and, subsequently, dried into a final gel-like structure.

The fabrication of PZT fibers in this work is outlined in Figure 1. As presented, two sources of the lead cation, lead (II) acetate trihydrate [Pb(CH₃COO)₂·3H₂O]* and lead (II) pentanedionate (lead acetylacetonte) [Pb(C₅H₇O₂)₂]† were used, the first having been initially employed[12], and the latter proposed to give a more stable PZT precursor solution.[13] For convenience, samples produced using lead acetylacetonate are designated "AcAc processed", and those using lead acetate trihydrate "Acetate processed". Based on the work by Blum and Gurkovich[14] and later by Budd et al.[15], zirconium n-butoxide [Zr(OBu)₄]* (80% solution in 1-butanol) and titanium isoproxide [Ti(OPrⁱ)₄]* were used as the zirconium and titanium sources, respectively. For niobium modified PZT, niobium ethoxide, [Nb(OC₂H₅)₅]† was added during the addition of the titanium precursor stage. Stoichiometric quantities of each chemical were weighed out in accordance with the PZT formulations $Pb(Zr_{0.48}Ti_{0.52})O_3$ and $Pb_{0.988}(Ti_{0.48}Zr_{0.52})_{0.976}Nb_{0.024}O_3$, as reported in Jaffe, Cook, and Jaffe[16].

A solution of 0.1 ml of water and 5 ml of 2-methoxyethanol was added to the various PZT precursors (0.02 M) containing 0.1 ml conc. HNO_3 to ensure condensation and hydrolysis reactions. The solution was concentrated by stirring at ~120°C and then cooled to ~40°C to form a viscous resin. *The spinnability of the sol was empirically determined by dipping a glass rod into the viscous medium and pulling up to draw a fiber.* A systematic rheological study is underway to determined the optimum viscosity range for fiber drawing.

The precursor solution was transferred to a vessel consisting of a spinneret and a plunger as shown schematically in Figure 2(a)[17]. Fibers were extruded through the spinneret with twelve 100 μm diameter holes at ~7 kPa of pressure. The spun-drawn fibers were collected on a rotation drum with a variable speed control, as described in Figure 2(b). Factors involved in controlling the diameter of the fibers are: (i) viscosity of the sol, i.e. control of hydrolysis and condensation reaction, (ii) spinneret diameter, and (iii) speed of the take-up drum.

Fibers with diameters ranging from 10 to 80 μm were fabricated. The fibers were dried at room temperature for approximately 12 hours, cut into lengths of ~10 cm and fired at temperatures from 750°C to 1250°C for 10 minutes. A heating rate of ~1°C/min. was used to allow the decomposition of organics being in the order of 10 to 15 wt% after solvent evaporation, which was previously determined by thermogravimetric analysis (TGA).[12] For samples fired at temperatures >1200°C, a lead atmosphere

---

* Aldrich Chemical Co., Milwaukee, WI.
† Johnson Matthey Catalog Co., Ward Hill, MA.

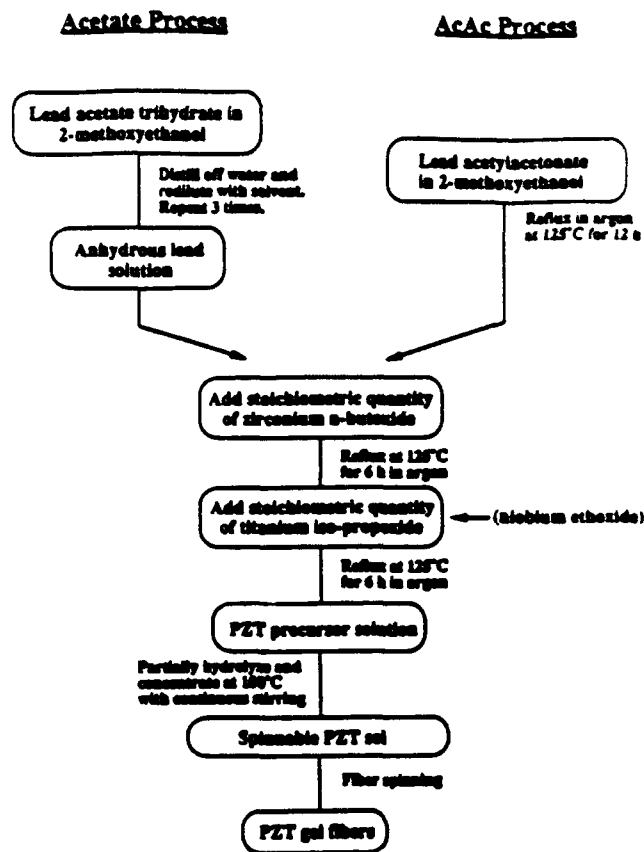Figure 1. Scheme for the preparation of Pb(Zr,Ti)O₃ fibers using lead acetate trihydrate (Acetate Process) and lead acetylacetonate (AcAc process) as a lead source.
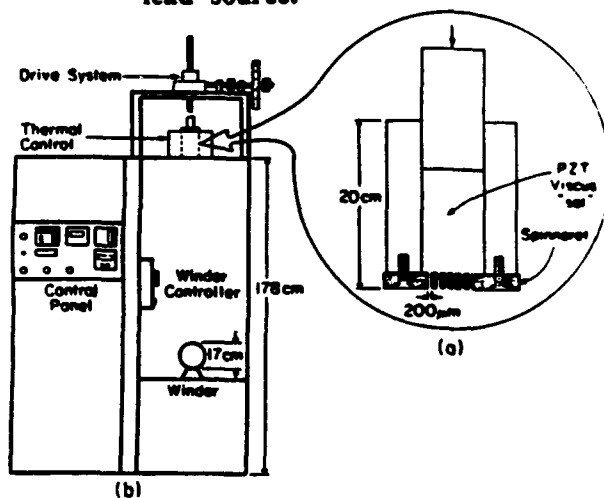

Figure 2. Fiber spinning apparatus. Schematic drawing of vessel and spinneret (a), and overview of the apparatus (b).

was created to minimize lead loss. The sintering condition of 750°C for 10 minutes was chosen based on a previous study[12] which was high enough to enable the formation of the desired perovskite structure, yet low enough to fire in open air without lead loss. This may be an important factor in the future when continuous fiber spinning and subsequent firing are desired. Firing temperatures at 1250°C were used to examine densification behavior and grain growth, being similar to that used for conventionally processed PZT ceramics.

2.2.   Characterization

Crystallinity and phase analysis of the fibers as a function of thermal treatment were determined using x-ray diffraction (XRD) analysis*. The microstructure, i.e. grain size and degree of porosity, and diameter of the fibers were examined using scanning electron microscopy (SEM)[†]. Energy dispersive spectroscopy (EDS)[§] was used to semi-quantitatively determine Zr:Ti and Pb:(Zr,Ti) ratios.

The room temperature dielectric properties (K @ 10 KHz) of sintered fibers were determined from capacitance measurements using a LCR meter and the holder presented in Figure 3. An external amplifier/divider circuit was employed to improve the sensitivity of the LCR meter[§] by a factor of 100 by increasing the applied signal to ~ 150 V_{rms}. A small amount of air-dry silver was applied to both ends of the fiber to ensure electrical contact. Fibers 1 to 2 cm and 20 to 30 μ in diameter in length were used. Because of the extreme geometry of these fibers, thus the very small capacitance of often less than 0.5 fF, very special care had to be taken to control the uniformity of the electric field within the three terminal parallel plate fixture. Because the capacitance to free space of even a short segment (under 20 μm) of fiber along its length can be greater than the end-to-end capacitance, it is critical that permittivity, as well as later described hysteresis measurements, be made in an environment with a controlled and, in this case, uniform electric field to avoid "shorting out" the measurement signal through an inadvertent T-network to ground. This is distinctly different from bulk or thin film measurements but is a crucial consideration in fiber measurements. Measurements were first made with the fiber in place then removed and the difference used as the sample's capacitance. This corrected for the contribution to the measured value from both stray capacitance and direct (air gap) capacitance. The diameter of the guard electrode (~ 5 cm) was chosen to ensure a uniform field in the neighborhood of the sample even with
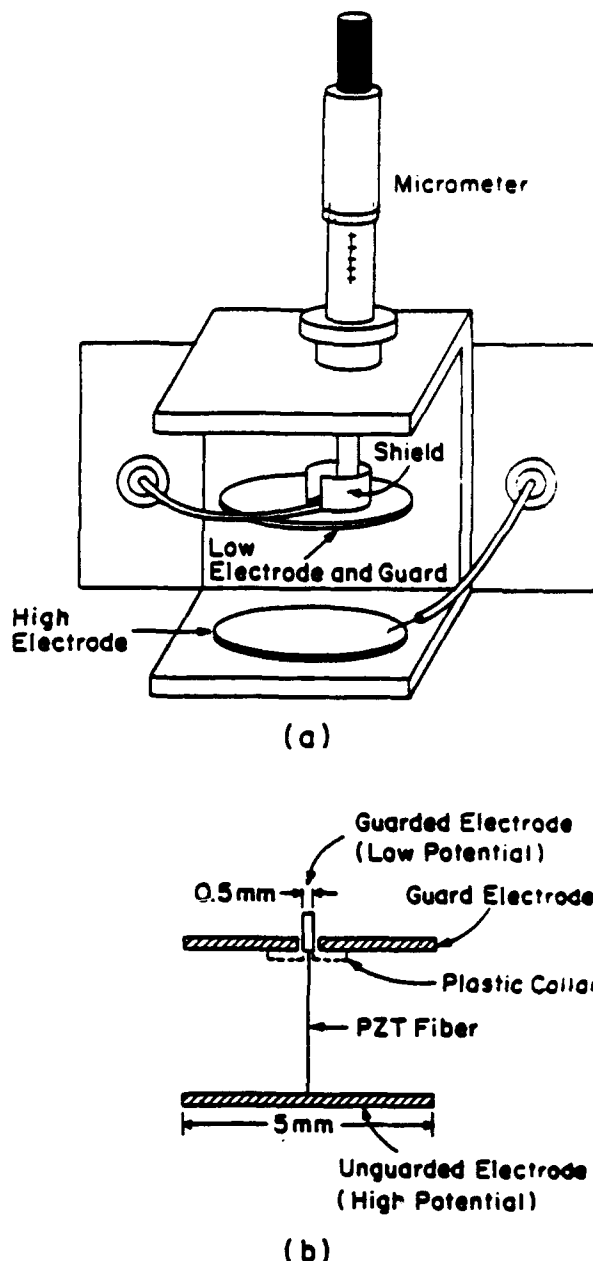

(a)

(b)

Figure 3.   **Fixture for fiber permittivity and polarization measurements (a), and section view of electrode configuration (b).**

the fibers ~ 2 cm in length. The size of the active low electrode in the fixture (0.5 mm in diameter) was calculated so that its contribution to the total capacitance would be no greater than that of even the smallest diameter fiber.

The ferroelectric nature of the fibers was confirmed through polarization E-field measurements with fibers only ~3 mm long, owing to voltage limitation of the power

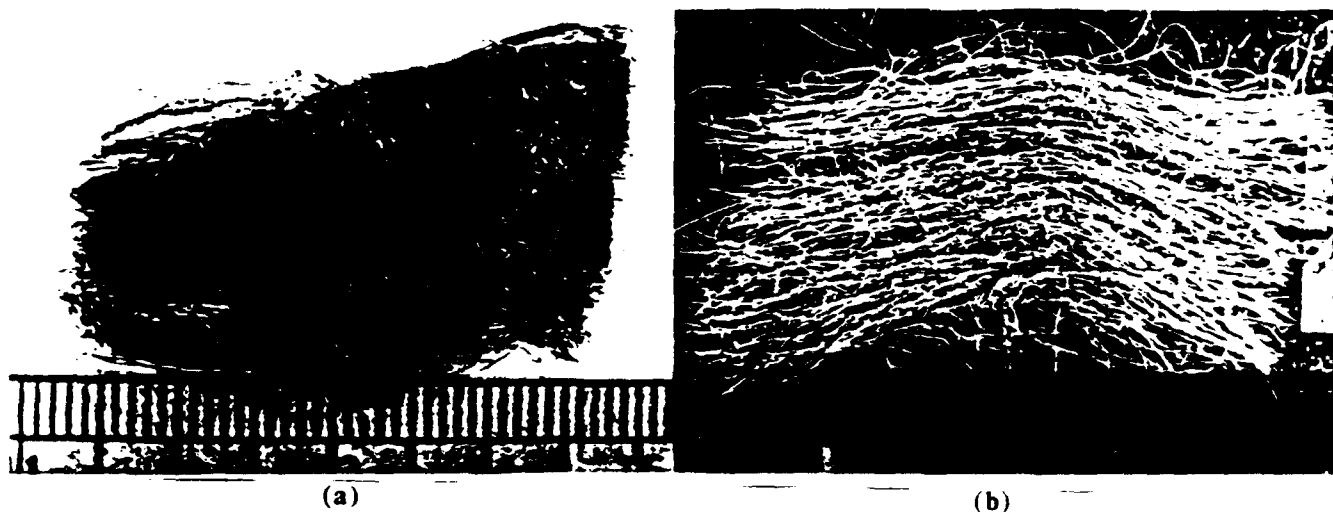**(a)**   **(b)**

Figure 4.   Photographs of (a) as spun, (b) fired PZT fiber.

supply*, i.e. 10 kV. A specially-built automated system was used which applies the excitation field and collects the charge while maintaining a virtual-ground state, similar to a classical Sawyer-Tower measurement, but the charge is collected by active circuitry rather than a passive capacitor. This holds the low side of the measurement circuit to within a few millivolts of ground, which is necessary to control the shape of the electric field for the same reason as in the permittivity measurement. To avoid electrical breakdown, the entire fixture was immersed in a fluorocarbon fluid†. Fields of > 3 MV/m, typically at a frequency of 10 Hz, were used.

To contrast both the physical and electrical characteristics of the fibers, disks (~1 cm in diameter) were prepared from gel-powders derived from the same sols used to draw fibers. Upon pressing and binder§ burnout, the disks were densified over a temperature range from 1000°C to 1400°C and characterized above. In addition to dielectric and polarization hysteresis, fully densified samples were polarized (poled) at 120°C with an electric field of 125 kV/cm. The level of poling was determined using a Berlincourt piezo d33 meter♦. The samples were allowed to age ~24 hours prior to measurement.

In addition to chemical and electrical characterization, the mechanical integrity of the PZT fibers was also investigated. The tensile strength was determined for selected fibers at the Nagasaki University of Japan, using a technique described by Iwanaga et al.[18] Specimens 1 to 2

---

*   High Voltage Power Supply, Model 610A, Trek
     Incorp., Medina, NY
†   Fluorinert FC-40, 3M Corp., St. Paul, MN
§   Polyvinyl Alcohol binder (PVA)
♦   Berlincourt Piezo d33 meter, Channel Products, Inc.,
     Chagrin Falls, OH

mm in length, diameter range between 26 to 36 μm, were glued to carbon fiber and the direct tensile strength was measured with a load range of 1 to 10g.

3.   RESULTS AND DISCUSSION

3.1.   Microstructural Analysis

Optical photographs of as-spun and fired fibers are shown in Figure 4(a) and (b), respectively. A representative XRD spectra of AcAc processed PZT fibers fired at 750°C and 1250°C are presented in Figure 5 revealing the presence of a well-crystallized perovskite phase. Figure 6 presents SEM micrographs of Acetate processed PZT, fired at (a) 750°C, (b) 1250°C, and Nb-PZT fired at 1250°C. As presented, the diameter of the fibers were in the range of 20 to 50 μm, showing little evidence of porosity on the surface of the fiber. The Acetate and AcAc (not shown in the figures) processed fibers fired at 750°C were found to possess similar microstructures. SEM examination of the cross section of the fibers revealed 10 to 20% fine porosity uniformly distributed across the fibers, except near the dense surface with grain sizes on the order of 0.2 - 0.3 μm. Fibers processed at 1250°C possessed dense microstructures and grain sizes in the range of 2 to 8 μm. A small amount of closed porosity (~ 0.3 μm in diameter), both in grains and at grain boundaries, was evident in the cross section view of the fiber after the pull test, as shown in Figure. The fracture surface was intergranular. The fibers with Nb-PZT (AcAc processed) composition fired at 1250°C were uniform and finer grain size, 1 to 3 μm, and little porosity. The smaller grain size is due to the niobium substitution which tends to inhibit grain growth of PZT in addition many other characteristics governed by this "A-site ... additive". Acetate processed Nb-PZT fiber could ...

drawn successfully, due to the rapid increase in "sol" viscosity. Differences between the two lead sources were inconclusive in this study, though use of lead acetylacetonate reduced reflux time drastically.

3.2. Compositional Analysis

EDS analysis of PZT fibers (both Acetate and AcAc processed) indicated that the Zr:Ti ratio was rich in Zr being shifted to approximately 55:45 as confirmed by the lack of tetragonal splitting ((002) and (200)) in the XRD patterns (Figure 5). This trend was confirmed by dielectric measurements of the fired pellets prepared from the same solution. The dielectric constant (K) dramatically decreased upon poling (~48%) reflecting a PZT composition well on the rhombohedral side of the morphotropic phase boundary (MPB).[16] The reason for this compositional shift is currently being investigated.

3.3. Electrical Properties

The dielectric constant values of the various fibers processed are summarized in Table I. Due to the small input signals, dielectric loss of the PZT fibers was not measured. Both Acetate and AcAc processed PZT fibers showed comparable dielectric values to that of the bulk ceramics disk samples made from the same solution. The dielectric constant of the samples fired at 750°C were lower, which was probably due to the combination of porosity and smaller grain size. Piezoelectric d_{33} coefficients of the PZT-poled ceramic disk samples were found to be ~150 pC/N, which is lower than reported value (~223 pC/N)[16]. This was believed to be due to the MPB compositional shifting of Zr:Ti. Poled ceramic disks of Nb-PZT exhibited d_{33} of ~350 pC/N close to the reported value (374 pC/N)[16]. Dielectric and piezoelectric properties of the bulk (disk) samples were necessary to determine the quality of precursors and to provide expected values for the fibers fabricated from the same "sol".

Representative room temperature hysteresis polarization E-field behavior for AcAc processed Nb-PZT fired at 1250°C is shown in Figure 8(a) along with the polarization measurements performed on bulk (disk) samples (Figure
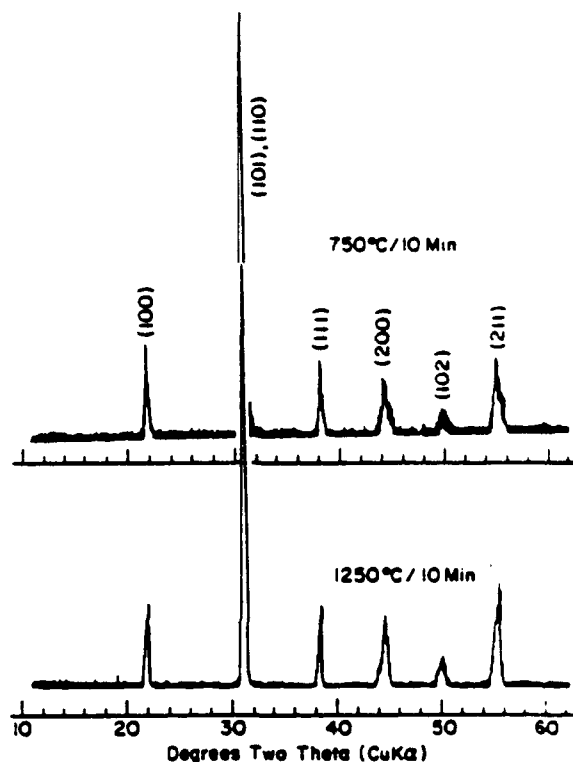

Figure 5. XRD pattern for the fibrousPZT heat-treated at 750°C for 10 min. and at 1250°C for 10 min.

Table I.   Dielectric Constant of Sol-Gel Derived PZT and Nb-PZT Fibers[a])

Ceramic	Pb Precursor	Heat Treatment Temp.[°C]/Time [min.]	Dielectric Constant (% error)
PZT	Acetate	750/10	670 (15)
"	"	1250/10	870 (10)
"	AcAc	750/10	500 (15)
"	"	1250/10	700 (10)
Nb-PZT	AcAc	750/10	1250 (15)
"	"	1250/10	1100 (15)

a) Fiber : Average diameter of 30 μm.
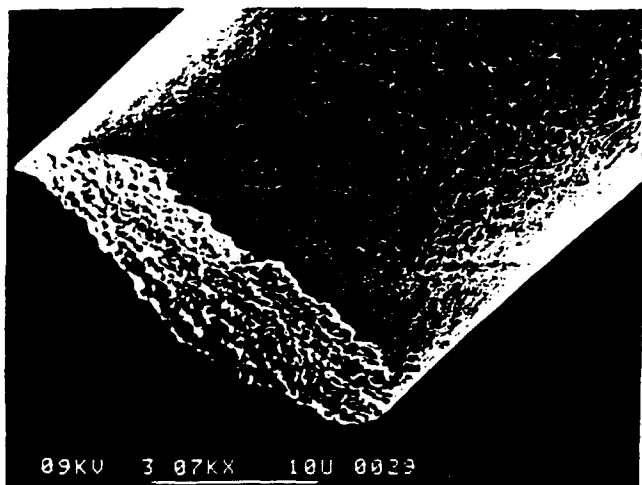
(a)
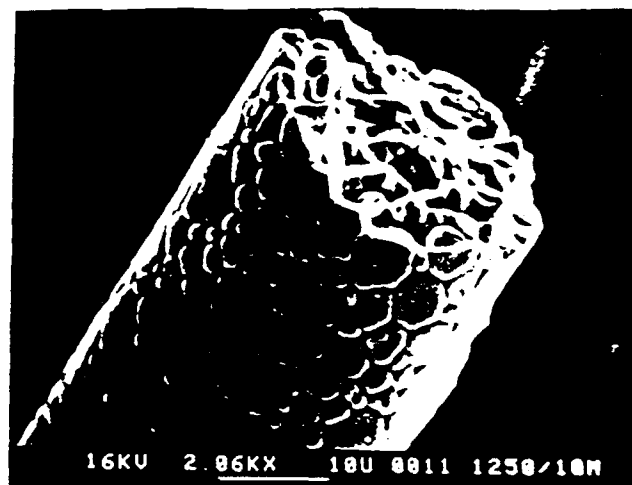
(b)

Figure 6. SEM micrograph of:
   (a)   Acetate processed PZT fired at 750°C for 10 min.
   (b)   Acetate processed PZT fired at 1250°C for 10 min.
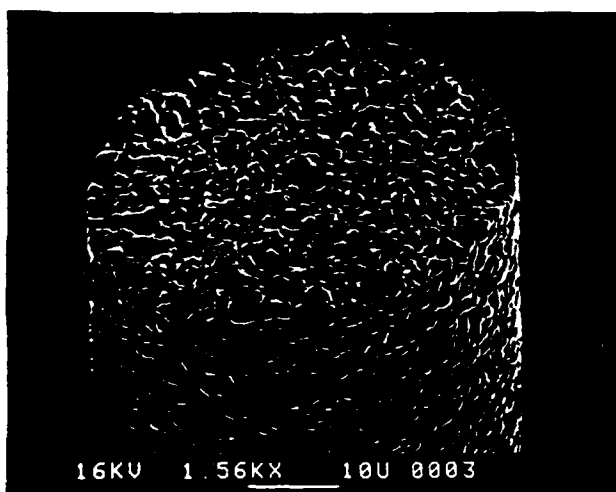

Figure 6. SEM micrograph of: (c)   AcAc
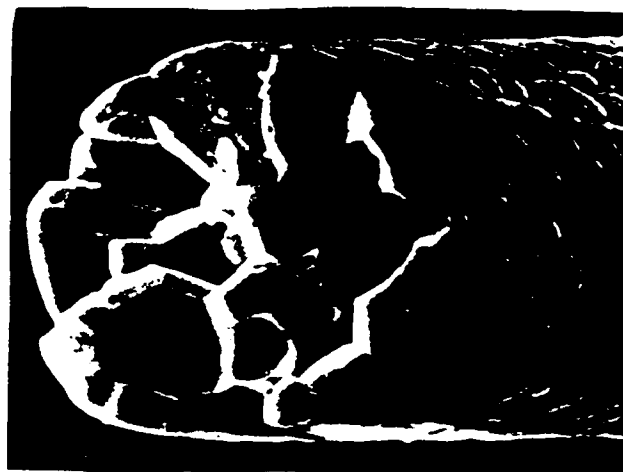   processed Nb-PZT fired at 1250°C
   for 10 min.

Figure 7. SEM micrograph of fracture surface of
   PZT fiber (fired at 1250°C for 10 min.
   after tensile test.

8(b)) as a comparison. Only Nb-PZT fiber data is presented due to the high coercive fields of unmodified PZT. The ferroelectric nature of a single piezoelectric fiber has not been reported before. The polarization hysteresis provides direct evidence that these fibers can be polarized to induce the desired piezoelectric properties. Comparison with the disk sample revealed that the level of remanent polarization of the fibers ($P_r = 37 \mu C/cm^2$) was similar to the bulk sample and coercive field was somewhat higher ($E_r = 19 kV/cm$).

3.4.   Mechanical Properties

Preliminary data for the tensile strength of PZT fibers fired at 750°C and 1250°C determined using the pull cut were 36 MPa and 40 MPa, respectively. Tensile strengths of ~55 MPa were found for Nb-PZT fibers. This higher value may be attributed to its smaller and more uniform grain size. Finer diameter fibers tended to give larger tensile strength values, though more data with different diameter samples is required to confirm this. Tensile strength values for bulk PZT ceramics reported in the literature is on the order of ~76 MPa[19], with modulus of
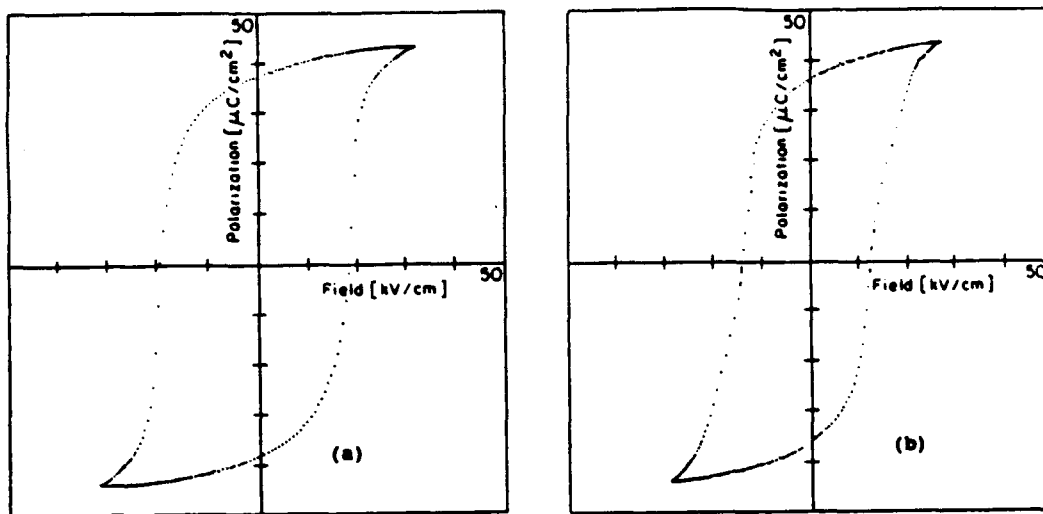
23

Figure 8. Polarization hysteresis of (a) Nb-PZT fiber (diameter 30 µm).
(b) Nb-PZT pellet prepared from the same sol as the fiber was spun.

rupture using 3-point flexure in the range of 10 to 40 MPa[20]. Therefore, the fiber tensile strength found for the fibers in this work is similar to that of the bulk ceramic. This range, however, is an order of magnitude less than comparable glass fibers (700 MPa) and substantially less than that for Al_2O_3 fibers (1500 MPa) reported in the literature[21]. Incorporation of PZT fibers into a structural matrix, therefore, cannot be a simple substitution with structural fibers, and hence careful handling and design must be considered.

4. CONCLUSIONS

Amorphous PZT and Nb-PZT fibers with average diameters of 30 µm have been successfully spin-drawn from sol-gel processed PZT precursor sol using a continuous batch spinning apparatus. Two different lead sources, lead acetate trihydrate and lead acetylacetonate, were examined. All of the fibers showed pure crystalline perovskite structure after heat treatment at 750°C, and further densification and grain growth were evident after 1250°C firing.

Single fiber dielectric constant and polarization hysteresis measurements were successfully performed using a specially built fixture. Dielectric constant values of the fibers fired at 750°C were lower than that of fibers fired at 1250°C due to porosity and reduced grain size. The dielectric constant of fibers fired at 1250°C was comparable with that of bulk ceramic values. Polarization E-field measurements of Nb-PZT fibers indicated that the level of remanent polarization (37 $\mu C/cm^2$) was similar to that of

bulk samples with the coercive field (19 kV/cm) being slightly higher.

Preliminary data for the tensile strength of PZT fibers revealed values similar to that of bulk PZT, though Nb-PZT fiber values were higher than that of pure PZT fibers, probably due to its denser microstructure and smaller, uniform grain size.

REFERENCES

1. E. Crawley and J. deLuis, "Use of Piezoelectric Actuators as Elements of Intelligent Structures," ACAA Journal, 25, 1373-1385 (1987).

2. A.R. Ramachandran, Q.C. Xu, L.E. Cross, and R.E. Newnham, "Passive Vibration Damping," First Joint U.S./Japan Conference on Adaptive Structures, Nov. 13-15, 1990, Maui, Hawaii, Proceeding ed. by B Wada, J.L. Fanson and K. Miura, Technomic

Publishing Co., Inc., Lancaster, PA (1991), pp. 523-528.

3. N.W. Hagood and A. von Flotow, "Damping of Structural Vibration with Piezoelectric Materials and Passive Electrical Networks," J. Sound and Vibrations 146, 243-268 (1991).

4. S. Yoshikawa, U. Selvaraj, K.G. Brooks, and S.K. Kurtz, "Piezoelectric PZT Tubes and Fibers for Passive Vibration Vibration Damping," IEEE, 8th International Symposium on Application of Ferroelectrics, Greenville, S.C., Aug. 30 - Sept. 2, 1992, Proceedings, pp. 269-272.

5. K.A. Klicker, J.V. Biggers, and R.E. Newnham, "Composite of PZT and Epoxy for Hydrostatic Transducer Applications," J. Am. Ceram. Soc., 64-65 (1981).

6. T.R. Gururaja, W.A. Schulze, T.R. Shrout, A. Safari, L. Webster, and L.E. Cross, "High Frequency Applications of PZT/Polymer Composite Materials," Ferroelectrics, 39, 1245 (1981).

7. H. Takeuchi and C. Nakaya, "PZT/Polymer Composite for Medical Ultrasonic Probes," Ferroelectrics, 68, 53 (1986).

8. H. Park, "PZT Fibers," ONR Review of Piezoelectric and Electrostrictive Material for Transducer Applications, State College, PA, April 22, 1991.

9. D.J. Waller, A. Safari, R. Card, and M.P. O'Toole, "Lead Zirconate Titanate Fiber/Polymer Composites Prepared by a Replication Process," J. Am. Ceram. Soc. 73, 3503-3506 (1990).

10. Vinay Seth, "Polycrystalline Ferroelectric Fiber," U.S. Patent #4,921,328, May 1, 1990.

11. Kuo-Chun Chen, Haixing Zheng, John D. Mackenzie, "Method for Making Piezoelectric Ceramic fibers," U.S. Patent #5,072,035, Dec. 10, 1991.

12. U. Selvaraj, A.V. Prasadarao, S. Komarneni, K. Brooks, and S.K. Kurtz, "Sol-Gel Processing of $PbTiO_3$ and $Pb(Zr_{0.52}Ti_{0.48})O_3$ Fibers," J. Mater. Res., 7, 992-996 (1992).

13. U. Selvaraj, K. Brooks, A.V. Prasadarao, S. Komarneni, R. Roy, and L.E. Cross, "Sol-Gel Fabrication of $Pb(Zr_{0.52}Ti_{0.48})O_3$ Thin Films Using Lead Acetylacetonate as the Lead Source," J. Am. Ceram. Soc. 76, 1441-44 (1993).

14. L.B.Blum and S.R. Gurkovich, J. Mater. Sci. 20, 4470 (1985).

15. K.D. Budd, S.K. Dey, and D.A. Payne, Brit. Ceram. Proc., No. 39, 107 (1985).

16. B. Jaffe, W.R. Cook, Jr., and H. Jaffe, "Piezoelectric Ceramics," pp. 135-83, Academic Press, New York, 1971.

17. G.J. Hayes, "Controlled Melt Spinning of Carbon Fiber," M.S. Thesis, Clemson University (1989).

18. H. Iwanaga, T. Iwasaki, K. Reizen, T. Matsunami, M. Ichihara, and S. Takeuchi, "Method for Tensile Experiments with Ceramic Fibers Having a Diameter of a Few Microns," J. Am. Ceram. Soc., 75, 1297-99 (1992).

19. Engineering Report, TP-226, Vernitron Piezoelectric Division.

20. R.C. Pohanka, P.L. Smith, and J. Pasternak, "Static and Dynamic Strength of Piezoelectric Materials," Ferroelectrics, 50, 285-291 (1983).

21. T.F. Cooke, "Inorganic Fibers--A Literature Review," J. Am. Ceram. Soc., 74, 2959-78 (1991).

APPENDIX B

Passively Damped Structural Composite Materials Using Resistively Shunted Piezoceramic Fibers

G.A. Lesieutre, S.Yarlagadda, S. Yoshikawa, S.K. Kurtz, and Q.C. Xu

The development of damped structural materials is an area of current research with potential for high rewards. Resistively shunted piezoceramic fibers used as reinforcement in a structural composite material offer the potential to significantly increase vibration damping capability. Available data indicate the predictable nature of this electroelastic damping mechanism, an important concern in design. This article addresses the current status of an effort to develop damped composites using resistively shunted piezoceramic fibers, including modeling aspects, performance limits, design guidelines, and fabrication issues. Initial design guidelines take the form of a modified modal strain energy method. With longitudinally poled fibers, peak damping loss factors of 12% are attainable in principle, even at relatively low (30%) piezoceramic fiber volume fractions. Some 30-μm diameter piezoelectric fibers have been produced using a sol-gel method, and details of poling and shunting are under investigation.

1. Introduction

THE use of piezoelectric materials with resistive shunting circuits to achieve passive vibration energy dissipation and resonant response reduction has been demonstrated by several researchers.[1-4] *Resistively shunted piezoceramics appear to offer several advantages over more conventional approaches to passive damping, including high stiffness and damping (loss modulus) for a potential composite constituent and tailorable frequency dependence.* A disadvantage includes the relatively high density of typical lead-base piezoceramics.

Because of high electroelastic coupling, the deformation of piezoelectric materials produces internal potential gradients. By placing electrodes on the material and shunting them through some finite resistance, current is allowed to flow, dissipating energy through joule heating.

When the dimensions of piezoelectric elements used for passive damping are comparable in magnitude to characteristic vibration lengths, element placement significantly affects achievable levels of structural damping. However, if the elements could be reduced in size and proliferated throughout a structure, possibly as reinforcement in a structural composite material, significant damping could be achieved with less sensitivity to placement.

This observation provided the motivation for the subject work, which addresses the development of resistively shunted piezoelectric ceramic fibers as a means to increase the vibration damping properties of structural composite materials to significant levels. Figure 1 shows a concept for such a fiber.

Key challenges identified at the outset of this effort were associated with fabrication and modeling. Fabrication issues included fiber production, poling, and electroding; provision of an integral, tailorable resistive path; and integration into a composite material. Modeling issues included estimation of achievable damping levels, shaping of frequency-dependent damping, and effects of complex stress states and shunting network topology. This article focuses on the modeling issues.

One of the primary goals of the modeling effort was an assessment of achievable damping performance. If initial estimates, based on simplified models, were to indicate that the levels of damping possible were not of engineering significance, there would be little motivation to proceed. If, on the other hand, further investigation was warranted, more detailed models would be needed to design composite materials for specific applications, as well as to guide continuing materials development.

The initial modeling effort concentrated on the development of simple models that could be used to establish possible performance levels. This was done using a two-step process. The first was to determine effective loss factors for the piezoelectric fiber; the second was to use those loss factors in the estimation of modal damping for flexure of a composite panel. The follow-

Electrodes

Fiber segment

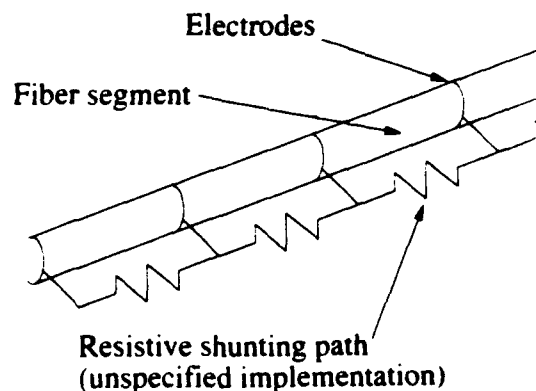**Resistive shunting path (unspecified implementation)**

Fig. 1 Resistively shunted piezoelectric fiber concept

G.A. Lesieutre, S.Yarlagadda, S. Yoshikawa, S.K. Kurtz, and Q.C. Xu, The Pennsylvania State University, University Park, PA 16802.

27

ing subsections discuss each of these steps in turn, as well as limitations of the models and future efforts.

2. Damping Performance Analysis: Effective Fiber Loss Factor

To a first approximation, the peak damping of a shunted piezoelectric fiber may be estimated by assuming that individual fibers in a composite experience a simple state of stress, namely pure longitudinal tension or compression, and that the stress is approximately uniform between two electrodes on the fiber. In this situation, the maximum damping achievable in the fiber alone may be treated as a material property—an effective longitudinal loss factor.

The damping of a composite material undergoing harmonic deformation may then be estimated as the sum of the damping in the constituent materials weighted by the relative contribution of each to total strain energy. Because the fiber modulus is typically much greater than that of the matrix material, most of the strain energy of deformation (often 80 to 95%) is found in the fiber. This is one of the primary motivations for seeking ways to increase the damping of reinforcing fibers.

As discussed in Ref 4, interpretation of the operative physical dissipation mechanism as an anelastic relaxation permits the use of classical relations for analysis (such as those discussed in Ref 5) and the extension of established tools for design purposes. In this approach, the difference between the low-frequency modulus (E_r, relaxed, short circuit) and the high-frequency modulus (E_u, unrelaxed, open circuit) is closely related to the peak material damping (η, loss factor) associated with that modulus. Equations 1a and 1b express both in terms of the relaxation strength, Δ:

$$E_u = E_r(1 + \Delta) \qquad [1a]$$

$$\eta = \frac{\Delta}{2(1 + \Delta)^{1/2}} \qquad [1b]$$

Note that the relaxation strength is closely related to the electromechanical coupling coefficient, k, as shown in Eq 2.

$$\Delta = \frac{k^2}{(1 - k^2)} \qquad [2]$$

The electroelastic relaxation strength corresponding to the longitudinal modulus may be found from consideration of the material constitutive equations, specialized to the case of a single non-zero (longitudinal) stress. The constitutive equations for a linear piezoelectric material relate the stress, T, and the electric displacement, D, to the strain, S, and the electric field, E, through several material properties. These properties include the elastic moduli, c^E, the piezoelectric constants, e, and the dielectric matrix, ε^S. Equation 3 shows the general form of the constitutive equations:

$$T = c^E S - e^t E$$

$$D = eS + \varepsilon^S E \qquad [3]$$

Note that the equations are expressed in compressed matrix form (as opposed to tensor form). For poled piezoceramic materials, the "3" direction is taken by convention to be the direc-

$$c^E = 10^{11} \times$$

1.2100	0.7540	0.7520	0	0	0
0.7540	1.2100	0.7520	0	0	0
0.7520	0.7520	1.1100	0	0	0
0	0	0	0.2110	0	0
0	0	0	0	0.2110	0
0	0	0	0	0	0.2260

$$e =$$

0	0	0	12.3000	12.3000	0
0	0	0	12.3000	12.3000	0
-5.4000	-5.4000	15.8000	0	0	0

$$\varepsilon^S = 10^{-8} \times$$

0.8107	0	0
0	0.8107	0
0	0	0.7345

tion of poling.

The material properties for PZT-5A,[6] of particular interest for this project, are (SI units):

The open circuit moduli, c^D, may be found by taking $D = 0$

$$c^D = c^E + e^t(\varepsilon^S)^{-1}e \qquad [4]$$

Similarly, the short circuit modulus may be found by taking $E_3 \equiv 0$. Note that, in practice, only the component of the electric field in the direction between the electrodes is zero.

If the case of longitudinal fiber poling is considered, and the only non-zero stress is T_3 (in the direction of poling, or along the fiber axis), then the corresponding moduli are found to be

(relaxed, E_3 short circuit) $E_r = 5.38 \times 10^{10}$ Pa

(unrelaxed, E_3 open circuit) $E_u = 10.41 \times 10^{10}$ Pa

The corresponding relaxation strength and loss factor for the longitudinal modulus are then:

(relaxation strength) $\Delta = 0.935$

(longitudinal loss factor) $\eta_L = 0.336$

Note that this approach yields a coupling coefficient, k_{11}, of 0.695, in agreement with the published value of 0.70.[6]

A similar approach (E_3 shorted) may be used to address the case of radial poling and longitudinal deformation or, equivalently, longitudinal poling and transverse deformation, to yield a value for the transverse loss factor:

(transverse loss factor) $\eta_T = 0.081$

Note that these values for η_L and η_T are ideal, peak loss factors attainable in practice over a limited frequency range. In composite design, other factors affecting the frequency-dependent

28

behavior must also be addressed. These factors include resistive shunting, nonuniform strain over finite fiber segment lengths, and shunting network topology. The following subsections briefly address the general effects of each of these factors.

2.1 Resistive Shunting

The dynamics of the electrical RC shunting network result in frequency-dependent behavior. However, the value of the shunt resistance(s) may be specified by a designer to tailor or "tune" the frequency dependence of damping to the application. Using the complex modulus representation of material properties $(E = E' + jE'')$, and assuming j multiple discrete electroelastic relaxations, the frequency dependence of the piezoceramic storage modulus, E', the loss modulus, E'', and the loss factor, η, are given by:[4]

$$E'(\omega) = E_r \left[1 + \sum_{i \text{ relaxations}} \Delta_i \frac{(\omega\tau_{\varepsilon i})^2}{1 + (\omega\tau_{\varepsilon i})^2} \right] \qquad [5a]$$

$$E''(\omega) = E_r \sum_{i \text{ relaxations}} \Delta_i \frac{(\omega\tau_{\varepsilon i})}{1 + (\omega\tau_{\varepsilon i})^2} \qquad [5b]$$

$$\eta(\omega) = \frac{E''(\omega)}{E'(\omega)} = \eta_{max} \frac{2(\omega\bar{\tau})}{1 + (\omega\bar{\tau})^2}$$

(for a single relaxation) $\qquad [5c]$

where $\tau_{\varepsilon i}$ is the ith characteristic relaxation time at constant strain, and $\bar{\tau}$ is the relaxation time (for a single relaxation):

$$\bar{\tau} = \tau_\varepsilon (1 + \Delta)^{1/2} \qquad [5d]$$

and $\tau_{\varepsilon i}$ is given by, for a single piezo segment:

$$\tau_{\varepsilon i} = R_i C_i^S \qquad [5e]$$

where R_i is the shunting resistance, and C_i^S is the capacitance at constant strain (between the two electrodes on the single segment).

2.2 Nonuniform Strain in Fiber Segments

If the strain within a fiber segment between adjacent electrodes changes sign within the segment, the effective loss factor approach to estimating damping is inappropriate. For example, consider the case of a sinusoidal strain distribution. If the wavelength is on the order of the segment length, no voltage appears across the electrodes, and as a result, no damping can occur. However, the effective loss factor approach would predict some damping based on the non-zero strain energy stored in the segment. In practice then, the fiber segment lengths must be considerably shorter than the smallest wavelength of vibration to be damped. Note that this effect is a result of the fact that, with external resistive shunting, piezoelectric damping is not

an intrinsic property of the material, but an extrinsic one, depending on structural length scales.

2.3 Shunting Network Topology

As noted in the preceding, the dynamics of the electrical shunting circuit results in frequency-dependent behavior. A circuit comprising a piezoelectric fiber (electrically a capacitor) and a shunt resistor exhibits characteristic exponential relaxation. The time constant of this RC circuit relaxation can be tuned to produce peak damping at a frequency of interest through the suitable selection of the shunt resistance.

For single-segment (monolithic) piezoelectric elements, this selection is fairly straightforward. For more complex circuits with multiple segments experiencing nonuniform strain, deformation of adjacent segments affects the electrical impedance "observed" at the terminals of a given segment. This factor should also be considered in design. Again, ensuring that fiber segment lengths are considerably shorter than the smallest wavelength of interest should minimize this effect.

3. Performance Analysis: Fiber Effectiveness in Composite Damping

The objectives of this part of the effort were (1) to develop a theoretical model for prediction of the modal damping of polymer/matrix composite plates with added resistively shunted piezoelectric fibers and (2) to use this model to assess the potential effectiveness of such fibers in damping plate vibrations. Previous study of the flexure of composite panels has shown that, in general, the reinforcing fiber (whatever the material) plays a significant role in damping "fiber-dominated" bending modes, but is less effective in damping "matrix-dominated" twisting modes.[7]

A two-part approach was followed in modeling composite plate damping. The first part involved micromechanical modeling to predict the stiffness and damping properties of a single composite lamina from fiber and matrix properties. The second part involved analytical dynamic modal analysis of a midplane-symmetric laminated composite plate.

3.1 Lamina Modeling

Several micromechanical models for calculating lamina elastic properties from constituent properties for two-phase composites are available in the literature. However, in this work the composite comprises three phases: reinforcing glass fibers, epoxy matrix, and resistively shunted piezoelectric fibers.

The three-phase composite of interest was treated as a two-phase material by considering the reinforcing fibers and matrix as an effective matrix phase and the piezoelectric fiber as the reinforcing phase. Properties of the effective matrix material were then calculated using micromechanical models valid for isotropic fibers in an isotropic matrix. Because of its two-phase nature, the resulting effective matrix is transversely isotropic.

The piezoelectric fibers also were treated as transversely isotropic, requiring the use of a micromechanical model that is valid for transversely isotropic fibers and matrix to determine

Table 1 Constituent material properties

	3M S2-glass fiber	Hercules 3501-6 epoxy
Young's modulus, E, GPa	86	4.0
Shear modulus, G, GPa	35	1.45
Poisson's ratio, v	0.22	0.38
Young's loss factor, η_E	0	0.03
Shear loss factor, η_G	0	0.033

Table 2 Composite plate configuration

Layup	Unidirectional
Geometry..........................	10 cm square, 2-mm thick (4-ply)
Boundaries........................	Cantilevered (CFFF) with fiber direction normal to clamped side

Fig. 2 Composite plate configuration.

lamina properties. One suggested scheme[8] was used to transform a micromechanical model for transversely isotropic fibers and an isotropic matrix[9] for use with transversely isotropic fibers and matrix.

The lamina elastic models described in the preceding were extended to include damping by representing material damping properties in terms of complex moduli. For harmonic forced vibration of a viscoelastic material, effective dynamic moduli can be determined from expressions for elastic moduli by allowing the elastic moduli to be complex.[10] The real part of a complex modulus is a measure of the stiffness of a material, whereas the complex part is a measure of damping.

3.1.1 Material Properties

Table 1 summarizes the properties used for the constituent materials in subsequent analysis.[11-13] Piezoelectric fiber damping was characterized by the (maximum) effective loss factors described in the preceding section. Note that the glass fiber has been assumed to be lossless, whereas the epoxy matrix exhibits substantial damping.

3.2 Plate Modal Analysis

The modal frequencies and damping of the composite plate were determined from lamina stiffness and damping properties, laminate stacking sequence and ply orientation, and plate geometry and boundary conditions. The approach used in this work is similar to that described in Ref 7, which contains additional references to other pertinent work. The following paragraphs provide an overview of the approach.

A higher order plate theory was used to include shear deformation and rotary inertia effects; appropriate terms appear in the expressions for plate strain and kinetic energy.

The Rayleigh-Ritz method was used to model the dynamic behavior of the plate under various boundary conditions. The assumed plate mode shapes for both transverse displacements and shear deformation were combinations of simple beam mode shapes that were appropriate to the boundary conditions. Use of these shapes with the strain and kinetic energy expressions and subsequent minimization yielded a complex matrix eigenvalue problem. The eigenvalues and eigenvectors were calculated using a standard complex eigenvalue extraction routine.
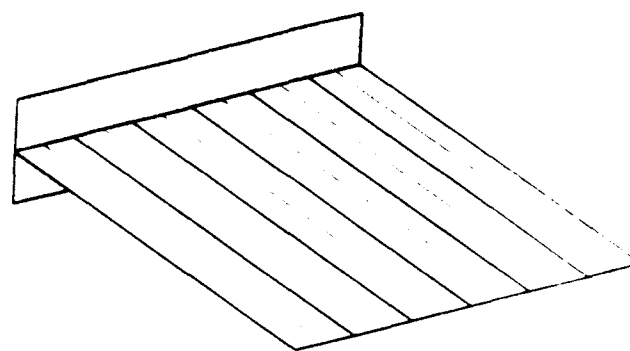
The resulting complex eigenvalues had the form:

$$\lambda = -\zeta\omega \pm i\omega\sqrt{1 - \zeta^2} \qquad (6)$$

from which the damped modal vibration frequency, $\omega\sqrt{}$ and modal damping ratio, ζ, were readily determined. Note that in the simplest case of a structure made from a single lightly damped material, the modal damping ratio is approximately half the material loss factor, η, at the corresponding frequency. An effective modal loss factor may thus be defined as twice the modal damping ratio.

3.2.1 Plate Configuration

Table 2 and Fig. 2 illustrate the baseline layup, geometry and boundary conditions considered in this analysis.

3.3 Results

The dependence of plate modal damping on piezoelectric fiber volume fraction was of particular interest in this study. Initially, the only piezoelectric damping of interest was that due to longitudinal stress, with a corresponding loss factor of 0.4 (longitudinal poling). Although it might seem straightforward to evaluate the damping of such composite materials assuming that the only non-zero damping loss factor is associated with longitudinal stress, such an approach would be incorrect. One result of such an assumption is a negative loss factor associated with some material deformation, which is not physically possible. This analysis used a non-zero loss factor associated with transverse deformation and assumed that it acted in addition to the longitudinal loss factor. For longitudinal fiber segmenting, the minimum value required was 0.05, whereas that determined from the material constitutive equations (with shorted) was 0.08.

This approach to combining damping associated with longitudinal and transverse deformation yields an upper bound the damping. Note that in practice, because each fiber segment has only a single pair of electrodes, transverse deformation may increase or decrease the potential difference between them, depending on the sign of the transverse stress would change the apparent damping, increasing or decreasing it according to the relative signs of the stresses. In general, the inclusion of transverse damping changed the results by less.

Table 3 Analysis cases for longitudinal fiber damping

Case No.	Piezo fiber	Volume fraction	
		Glass fiber	Epoxy matrix
0	0	0.6	0.4
1	0.1	0.5	0.4
2	0.2	0.4	0.4
3	0.3	0.3	0.4

Table 4 Elastic properties of 0 and 30% piezo lamina

	Case 0	Case 3
Longitudinal modulus, E_L, GPa	53.2	43.4
Transverse modulus, E_T, GPa	13.5	13.7
Shear modulus, G_{LT}, GPa	5.0	5.2
Transverse shear modulus, G_{TT}	4.5	4.6
Poisson's ratio, v_{LT}	0.28	0.33
Density, ρ, kg/m^3	2006	3581

Table 5 Modal loss factors for 0% and 30% piezo lamina

Mode	Case 0	Case 3	Increase, %
1	0.0018	0.1230	6730%
2	0.0167	0.0684	310%
3	0.0240	0.0354	48%
4	0.0021	0.1210	5660%
5	0.0078	0.0977	1150%
6	0.0250	0.0624	150%

Fig. 3 Modal vibration frequencies versus mode number and piezo volume fraction case.

Fig. 4 Modal loss factors versus mode number and piezo volume fraction case.

to 3%. A more detailed analysis of the effects of complex stress states would likely require a numerical coupled field approach, perhaps like that described in Ref 14.

In all of the cases considered, the epoxy matrix volume fraction was assumed to be fixed at 0.40, whereas the remaining 0.60 was divided between glass fiber and resistively shunted piezoelectric fiber. A reasonable upper limit on piezoceramic volume fraction was taken as 0.30. Table 3 summarizes the initial analysis cases considered.

Table 4 summarizes the calculated elastic properties for cases 0 and 3 (0 and 30% piezo, respectively). Note that the addition of 30% piezoceramic fiber decreases the plate longitudinal (short circuit) stiffness by 18% and increases the density by 79%. Clearly, large increases in damping are needed to justify the use of piezoceramic fibers in a glass/epoxy composite structure.

Figures 3 and 4 show the dependence of composite plate vibration frequencies and damping on piezoelectric fiber volume fraction. Note that the modal frequencies generally decrease with the addition of piezoceramic fiber and that the modal loss factors increase dramatically.

The frequencies decrease because the density increases and the stiffness decreases. With the addition of 30% piezoceramic fiber, the largest frequency change is 31%, whereas the smallest is 25%. By sensitivity, the modes are ordered 1, 4, 5, 2, 6, and 3. Mode 1 is a fiber-dominated bending mode, whereas mode 3 is a matrix-dominated twisting mode. The behavior of the other modes is between these extremes.
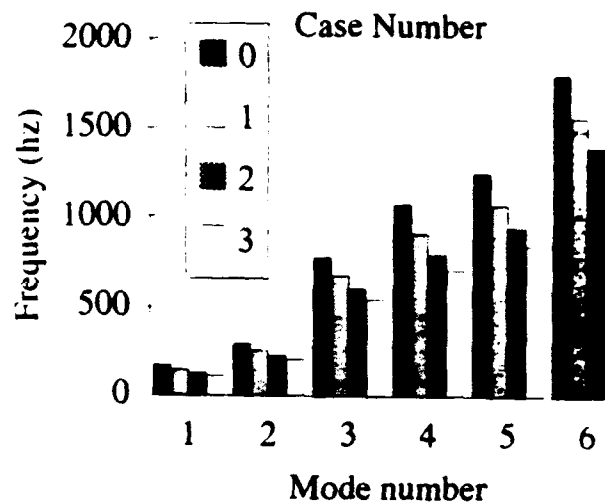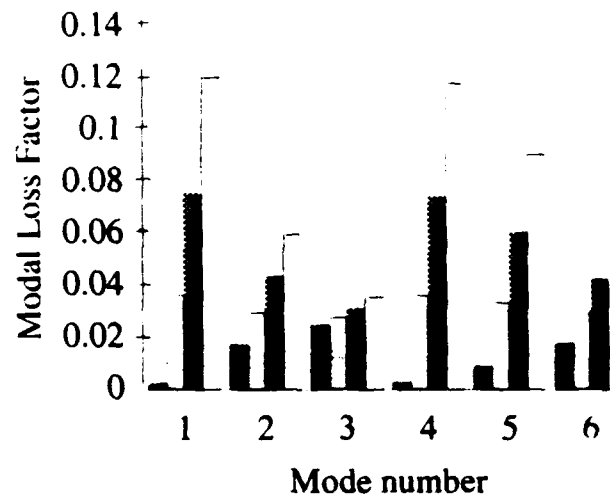
Table 5 summarizes the effective modal loss factors for cases 0 and 3 (0 and 30% piezo, respectively), along with the percentage changes in damping. With the addition of 30% piezoceramic fiber, mode 1 damping increases by a factor of a level of over 12%. Mode 3 is affected the least, but nevertheless increases by 50% to a level of 3.5%. This result is consistent with previous findings regarding the role of the fiber composite damping.[7] Note that, for nonunidirectional arrangements and for shell-type structures that carry in-plane loads, fiber damping would play an important role in most vibration modes.

Additional cases were also considered, including both longitudinal and radial poling of piezo-coated glass fibers. In cases, the dominant contributor to increased composite damping was the loss factor associated with longitudinal fiber deformation. This is primarily the result of the high participation composite modal strain energy.

3.4 *Experimental Results*

Experimental results validating the general concept of shunted piezoelectric damping using monolithic elements (including small, 1-mm diam, PZT tubes) have been reported in the literature.[1-4] No fine-scale resistively shunted piezoelectric fiber composites have been constructed to date, although work on such materials is in progress.

4. Piezoelectric Fiber Fabrication

Researchers have recently fabricated 30-μm diameter PZT fibers ($PbZr_{0.52}Ti_{0.48}O_3$) from viscous spinnable solutions prepared by sol-gel processing of alkoxide precursors. Following heat treatment, these fibers were found to consist of fully dense submicron grains and to exhibit dielectric constants of 800. This progress is discussed in detail in Ref 15.

The additional critical aspects of fiber electroding, poling, and integral shunting are currently under investigation. Various alternative approaches are being considered for each.

5. Summary and Conclusions

In summary, there is a need for structural materials with enhanced intrinsic vibration damping capability. Although researchers have recently demonstrated the use of resistively shunted piezoelectric materials to increase structural damping, these efforts used elements with dimensions on the same order as those of structural elements. The extension of this emerging research area to composite materials with tailorable frequency-dependent damping, along with corresponding design and analysis tools, shows promise. With longitudinally poled fibers, peak modal loss factors of 12% are theoretically attainable in a PZT/S-glass/epoxy composite, even at relatively low (30%) piezoceramic fiber volume fractions.

To the extent practical, piezoelectric fiber material should be poled longitudinally to attain the maximum damping; the form of the material (coating versus separate fiber) is unimportant. Successful pursuit of this avenue of development would mark a significant advance in the technology of engineered structural materials.

References

1. N.W. Hagood and A.H. von Flotow, Damping of Structural Vibrations with Piezoelectric Materials and Passive Electrical Networks, *J. Sound Vibration*, Vol 146, 1991

2. S. Yoshikawa, U. Selvaraj, K.G. Brooks, and S.K. Kurtz, "Piezoelectric PZT Tubes and Fibers for Passive Vibrational Damping," Proc. ISAF Conf., Greenville, SC, Aug 31, 1992

3. D. Edberg, A.S. Bicos, C.M. Fuller, J.J. Tracy, and J.S. Fechter, Theoretical and Experimental Studies of a Truss Incorporating Active Members, *J. Intelligent Mater. Sys. Struct.*, Vol 3, 1992, p 333-347

4. C.L. Davis and G.A. Lesieutre, A Modal Strain Energy Approach to the Prediction of Resistively-Shunted Piezoceramic Damping, *J. Sound Vibration*, submitted for publication

5. A.S. Nowick and B.S. Berry, *Anelastic Relaxation of Crystalline Solids*, Academic Press, 1972

6. D. Berlincourt, H.H.A. Krueger, and C. Near, "Important Properties of Vernitron Piezoelectric Ceramics," Engineering Report TP-226, Vernitron Piezoelectric Division, Bedford, OH

7. S. Yarlagadda and G.A. Lesieutre, Fiber Contribution to Modal Damping of Polymer Matrix Composite Panels, *J. Spacecr. Rockets*, in press

8. Z. Hashin, Analysis of Composite Materials—A Survey, *J. Appl. Mechan.*, Vol 50, 1983, p 481-491

9. S.K. Datta, H.M. Ledbetter, and R.D. Kriz, Calculated Elastic Constants of Composites Containing Anisotropic Fibers, *Int. J. Solids Struct.*, Vol 20, 1984, p 429-438

10. Z. Hashin, Complex Moduli of Viscoelastic Composites General Theory and Application to Particulate Composites, *Int. Solids Struct.*, Vol 6, 1970, p 539-552

11. 3M S-glass Product Information, 3M Structural Products Department, St. Paul, MN, 1992

12. Hercules Epoxy Resin 3501-6 Product Data, No. 865, Hercules Inc., Wilmington, DE

13. G.A. Lesieutre, S. Yarlagadda, D. Christiansen, and W. Whatley, Enhanced Composite Plate Damping using Intercalated Graphite Fiber, *AIAA J.*, Vol 31, No. 4, 1993, p 746-750

14. G.A. Lesieutre, Finite Elements for Dynamic Modeling Uniaxial Rods with Frequency-Dependent Material Properties, *Int. J. Solids Struct.*, Vol 29, 1992, p 1567-1579

15. U. Selvaraj, A.V. Prasadarao, S. Komarneni, K.G. Brooks and S.K. Kurtz, Sol-Gel Processing of $PbTiO_3$ and $Pb(Zr_{0.52}Ti_{0.48})O_3$ Fibers, *J. Mater. Res.*, Vol 7, 1992, p 992